

Photo-induced dynamic association of coumarin pendants within amphiphilic random copolymer micelles

Huan Chang · Yan Liu · Mei Shi · Zhaotie Liu ·
Zhongwen Liu · Jinqiang Jiang

Received: 16 September 2014 / Accepted: 25 November 2014 / Published online: 4 December 2014
© Springer-Verlag Berlin Heidelberg 2014

Abstract The water-soluble amphiphilic random copolymer of P(DMA-*co*-VBC) with coumarin pendants has been designed to investigate the photo-induced dynamic association of coumarin pendants within polymer micelles in aqueous solution. Methods of absorption and emission spectra, solution transmittance, dynamic light scattering (DLS), and atomic force microscope (AFM) were applied. It was found that P(DMA-*co*-VBC) can form polymer micelles in aqueous solution. The time-dependent photo-dimerization degree (PD) of polymer micelles upon different intensity irradiations of 320 nm light showed saturating behaviors with an intensity-independent value of the maximum photo-dimerization extent, while the maximum photo-cleavage extent of coumarin dimers declined with the increasing intensity of 254 nm irradiation at used conditions. Furthermore, a significant emission band at 445 nm (I_2) evidently emerged as against the disappearance of emission band at 385 nm (I_1) during the photo-dimerization, and the time-dependent I_2/I_1 ratios of polymer aqueous solution upon alternative irradiations of 320 and 254 nm light showed a wave-like increase as a function of irradiation cycles, indicating a wavy closeness of coumarin pendants within polymer micelles during the reversible photo-dimerization cycles.

Keywords Amphiphilic polymer · Micelles · Coumarin · Reversible photo-dimerization · Hydrophobic association

Electronic supplementary material The online version of this article (doi:10.1007/s00396-014-3474-7) contains supplementary material, which is available to authorized users.

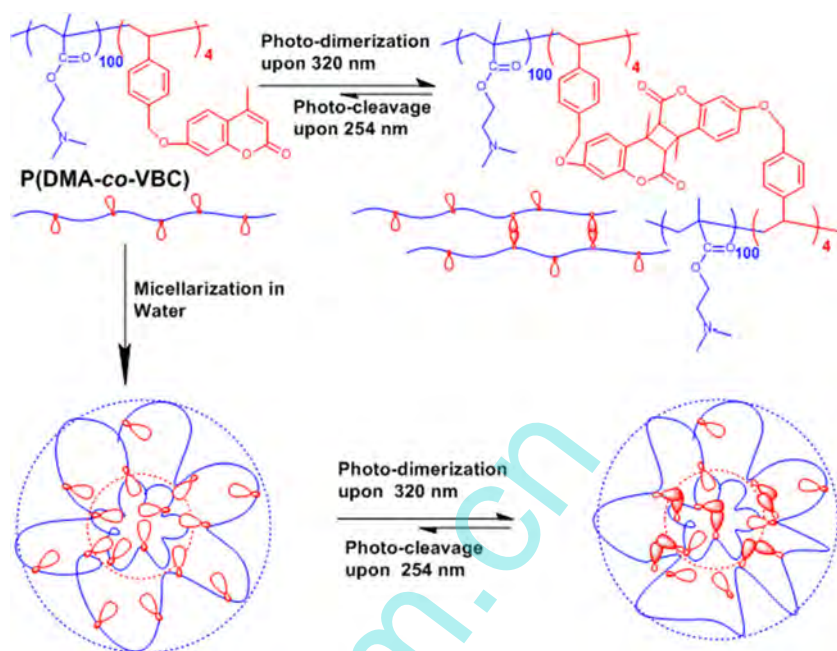
H. Chang · Y. Liu · M. Shi · Z. Liu · Z. Liu · J. Jiang (✉)
Key Laboratory of Applied Surface and Colloid Chemistry, Ministry of Education, School of Chemistry and Chemical Engineering, Shaanxi Normal University, Xi'an, Shaanxi 710062, China
e-mail: jiangjq@snnu.edu.cn

Introduction

Water-soluble amphiphilic copolymers (WSAPs) have attracted much attention in the past years due to their unique self-assembly behaviors upon various chemical and physical stimuli, such as pH, temperature, light, and redox [1–4]. Like amphiphilic block copolymers, WSAPs can self-assemble into various nano-aggregates, which can be exploited for potential applications in nano-carriers, nano-reactors, etc. [5–14]. A simplest design of WSAPs is to introduce a small amount of hydrophobic comonomers into the water-soluble polymer. To be emphasized, due to the unique random sequence architecture, this design would allow the objected polymer to self-assemble loosely in aqueous solution with hydrophobic components associating gradually from outside to inside and to move toward a certain direction upon external stimuli. Further understanding on their micellization and stimuli-responsive behaviors may improve their opportunities in potential applications.

Coumarin and its derivatives have attracted considerable attention because of their diverse photophysical and photochemical properties [15–18]. In addition, coumarins can undergo a 2+2 photo-dimerization upon irradiations at $\lambda > 300$ nm and then revert to the starting compound upon irradiations at $\lambda < 300$ nm [19]. Since this reversible photo-dimerization was first disclosed in 1902 [19], enormous studies concerning coumarins have been published due to their unique photochemistry [20–25]. Moreover, in recent years, applications of this reversible reaction have been explored where coumarins can be used as phototriggers for light-sensitive amphiphilic polymers. Here, as illustrated in Scheme 1, we used the water-soluble amphiphilic random copolymer of poly[2-(dimethylamino) ethyl methacrylate-*co*-7-(4-vinyl-benzoyloxy)-4-methylcoumarin] (P(DMA-*co*-VBC)) to investigate its micellization in aqueous solution and the reversible photo-dimerization of coumarin pendants

Scheme 1 Schematic illustration of the water-soluble amphiphilic random copolymer of P(DMA-co-VBC) and its reversible photo-dimerization upon alternative irradiation in aqueous solution



within polymer micelles upon alternative irradiations of 320 and 254 nm light.

Experimental section

Materials

Ethyl-2-bromo-2-methylpropionate (EBM-Br), *N, N, N', N', N'*-pentamethyl-diethylenetriamine (PMDETA), Cu(I)Br, 4-vinylbenzyl chloride (90 %), 7-hydroxy-4-methylcoumarin, 4-methoxyphenol (99 %), 2-(dimethylamino) ethyl methacrylate (DMAEMA), anhydrous potassium carbonate, and neutral Al₂O₃ were purchased from Aladdin. DMAEMA was passed through a neutral Al₂O₃ column to remove the inhibitor before the polymerization. 7-(4-Vinyl-benzyloxy)-4-methylcoumarin (VBC) was prepared according to previous works [26, 27].

Characterization

¹H-NMR spectrum (400 MHz) was investigated by a Bruker spectrometer with CDCl₃ as solvent. Gel permeation chromatography (GPC) was performed using a Waters system equipped with a refractive index and a photodiode array detector using THF as eluent (0.5 mL/min) and polystyrene standards for calibration.

Dynamic light scattering (DLS) measurements were performed at 25 °C with a Malvern Nano-ZS90 instrument (Malvern, UK) to determine the average diameter and size distribution of polymer micelles. Fluorescent emission spectra were recorded on a QuantaMaster™ steady-state fluorometer

(PTI, America) at 25 °C. UV–vis absorption spectra were recorded on a UV-6100s Spectrophotometer (Shanghai Meipuda Instrument Co., Ltd., China) at 25 °C. Atomic force microscope (AFM) images of micelles were obtained in tapping mode on a CSPM5500A scanning probe microscope system (Beijing Benyuan Nanometer Instrument Co., Ltd., China). The samples were prepared by dropping the micellar solution (2.50×10^{-2} mg/mL) onto mica sheet and dried at room temperature overnight.

Polymer preparation

In the polymerization, EBM-Br initiator (0.058 g, 0.3 mmol), Cu(I)Br (0.086 g, 0.6 mmol), DMAEMA (5.030 g, 32 mmol), VBC (0.750 g, 2.5 mmol), PMDETA (0.110 g, 0.6 mmol), and dioxane (10 mL) were quickly added into a 50-mL ampoule. Then, the mixture was degassed three times using the freeze-pump-thaw procedure and sealed under vacuum. After 30 min stirring at room temperature, the ampoule was placed in a preheated oil bath (60 °C) for 24 h. Then, the solution was passed through a neutral Al₂O₃ column with chloroform as eluent to remove all the catalyst. The amphiphilic random copolymer of P(DMA-co-VBC) was collected by precipitation twice into ethyl ether. The pale yellow powder was dried under vacuum at 30 °C overnight (yield, 70 %; Mn = 1.67×10^4 g/mol; Mw/Mn = 1.20 (GPC)).

In order to determine the critical micelle concentration (CMC) value of P(DMA-co-VBC) in aqueous solution, calculated concentrations of polymer in previously pyrene-saturated aqueous solution were excited at 334 nm, and the CMC value at 4.70×10^{-3} mg/mL was determined according

to the I_1/I_3 ratio changes as a function of polymer concentration.

Reversible photo-dimerization experiments of P(DMA-*co*-VBC) in aqueous solution

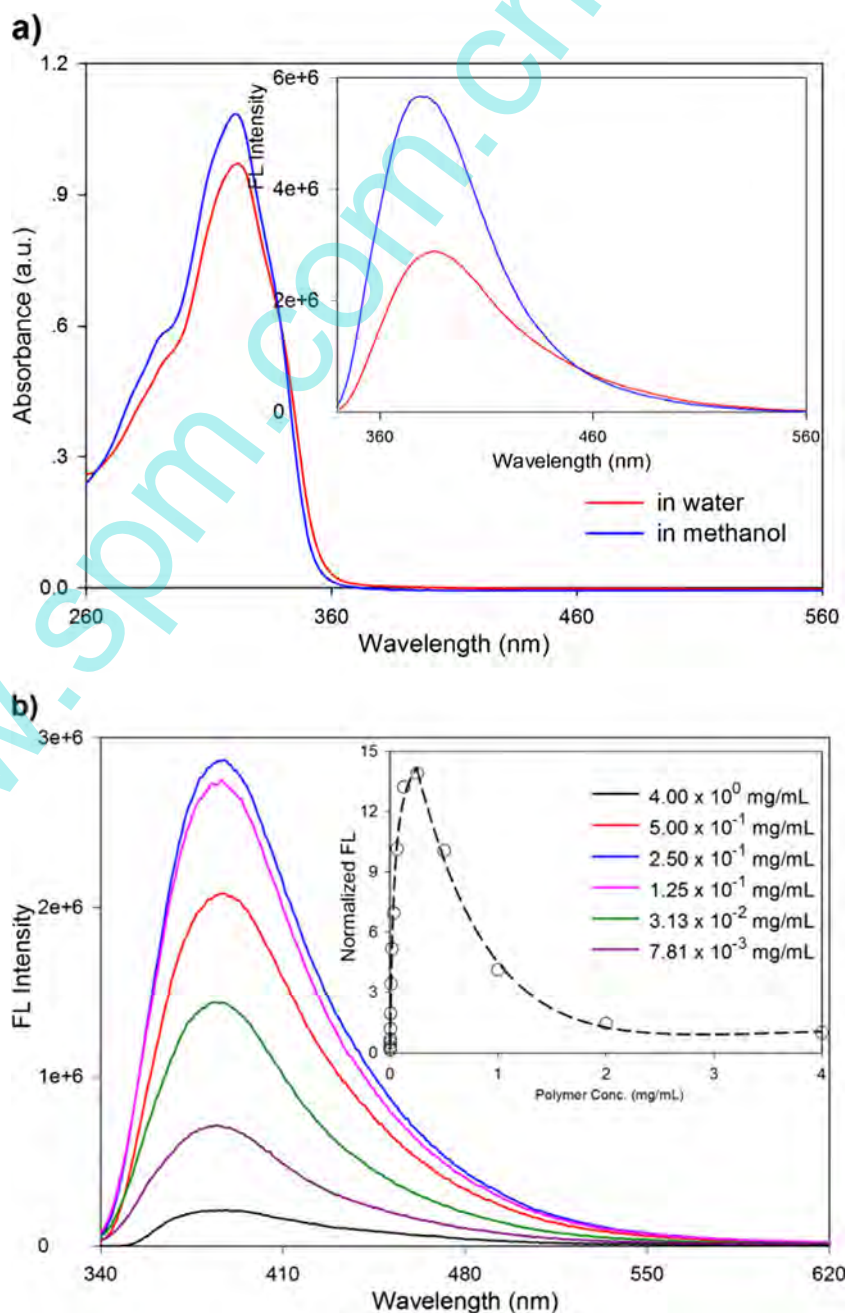
The alternative narrow band of light at 320 and 254 nm was derived from an adjustable double grating monochromator of Omni- λ 1805i equipped with a broadband laser-driven light of EQ-1500 LDLSTTM and a set of six optical filters.

The calculated amount of P(DMA-*co*-VBC) was directly dissolved into deionized water to get a concentration of

0.25 mg/mL. For the photo-dimerization experiment, 1 mL of polymer micellar solution was sealed in the fluorescent cuvette and irradiated by 320 nm light with different intensities, and for the photo-cleavage procedure, the polymer aqueous solution was first photo-dimerized to the given dimerization extent (88.31 %) with 320 nm light (0.86 mW/cm^2), then irradiated by 254 nm light with different intensities. The distance between the quartz wall and the spot light was 0.2 cm, and light intensities at the cuvette surface were measured by a CEL-NP 2000 optical power meter.

For the reversible photo-dimerization procedure, polymer aqueous solution ($0.25 \text{ mg/mL} \times 1 \text{ mL}$) was alternatively

Fig. 1 **a** Absorption and emission spectra ($\lambda_{\text{ex}}=320 \text{ nm}$) of polymer (0.25 mg/mL) in water and methanol, respectively. **b** Emission spectra ($\lambda_{\text{ex}}=320 \text{ nm}$) of polymer aqueous solution; the *inset* showed the normalized FL changes as a function of polymer concentration



irradiated by 320 nm (0.86 mW/cm^2 , 50 min) and 254 nm (0.24 mW/cm^2 , 90 min) for four cycles to evaluate their reversibility.

In order to check the changes of micellar size and solution transmittance during the reversible photo-dimerization, a thicker polymer aqueous solution ($5.0 \text{ mg/mL} \times 1.5 \text{ mL}$) was also alternatively irradiated with 320 nm (0.86 mW/cm^2 , 200 min) and 254 nm (0.24 mW/cm^2 , 150 min) for four cycles. The solution transmittance at 621 nm was collected by UV-vis instrument in transmittance mode. The micelle size changes were monitored with DLS. The irradiation cycles were also monitored with absorption spectra to make sure that the final photo-dimerization degree in every photo-reaction stage was almost the same with that of the dilute solution (0.25 mg/mL) upon alternative irradiations respectively.

The photo-dimerization degree (PD) was calculated from the UV-vis spectra by comparing the peak absorption at 320 nm assigned to the coumarin group by the following equation:

$$\text{PD}(\%) = 100 \times (A_0 - A_t) / A_0 \quad (1)$$

Here, A_0 and A_t were the absorbance intensities at 320 nm. 0 and t represented before and after the t time of irradiation, respectively.

Results and discussions

The micellization of P(DMA-co-VBC) in aqueous solution

As shown in Fig. 1a, P(DMA-co-VBC) in methanol and water gave similar $n \rightarrow \pi^*$ absorptions around 320 nm, and the

absorption intensity in methanol was slightly higher than that in water. However, the emission intensity at 385 nm ($\lambda_{\text{ex}} = 320 \text{ nm}$) in water was very much suppressed than that in methanol, indicating the possibility of hydrophobic association of coumarin pendants in aqueous solution. As shown in Fig. 1b, the emission spectra of polymer aqueous solution at different concentrations exhibited nearly no significant peak shift. However, as shown in the inset of Fig. 1b, the normalized maximum emission peak at 385 nm was not always strengthening as a function of polymer concentration, which was strengthened at the beginning ($< 2.50 \times 10^{-1} \text{ mg/mL}$) and then became weak with the increasing polymer concentration. This phenomenon was often found in assemblies of coumarin-containing polymers. The self-quenching effect of coumarin decreases with the decreasing polymer concentration first, then the fluorescence decreases with the further dilution.

In order to verify the micellization of P(DMA-co-VBC) in aqueous solution, the objected polymer was dissolved in previously pyrene-saturated aqueous solution and monitored with pyrene probe technique. As shown in Fig. 2, the emission spectra ($\lambda_{\text{ex}} = 334 \text{ nm}$) exhibited a vibrational fine five peaks emission of pyrene at the beginning ($< 1.25 \times 10^{-1} \text{ mg/mL}$), which was then suppressed to a broad emission band covering 350–550 nm interval with the increasing polymer concentration. The inset in Fig. 2 showed the intensity ratio of the first (I_1 at 373 nm) and third peaks (I_3 at 384 nm) as a function of polymer concentration; the dependence of I_1/I_3 on the polymer concentration below $4.70 \times 10^{-3} \text{ mg/mL}$ remained constant and then decreased progressively, which reflected the onset of micellar formation and the partitioning of the pyrene between the aqueous and micellar phases [28–30]. Therefore, the CMC value for P(DMA-co-VBC) in aqueous solution could be determined as $4.70 \times 10^{-3} \text{ mg/mL}$. Taking both the

Fig. 2 The emission spectra ($\lambda_{\text{ex}} = 334 \text{ nm}$) of polymer in previously pyrene-saturated aqueous solution; the inset showed the dependence of I_1/I_3 as a function of polymer concentration

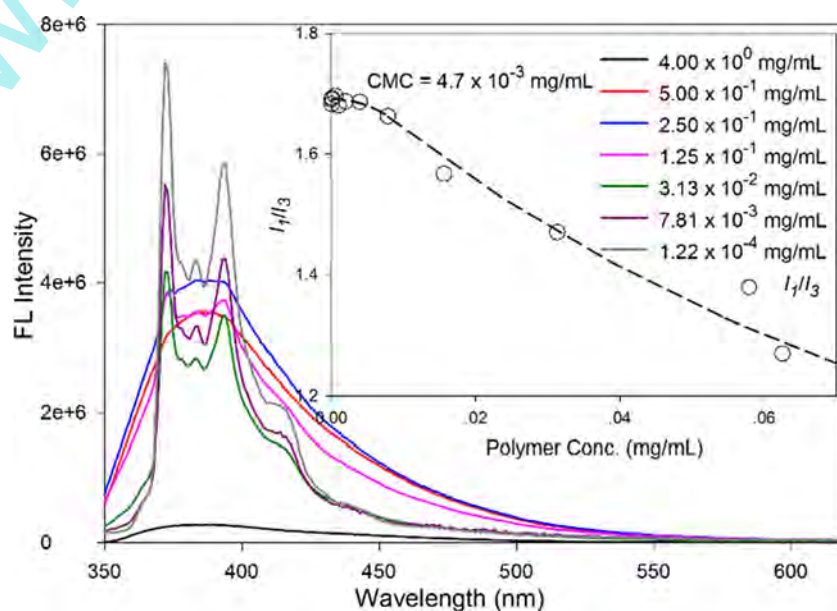
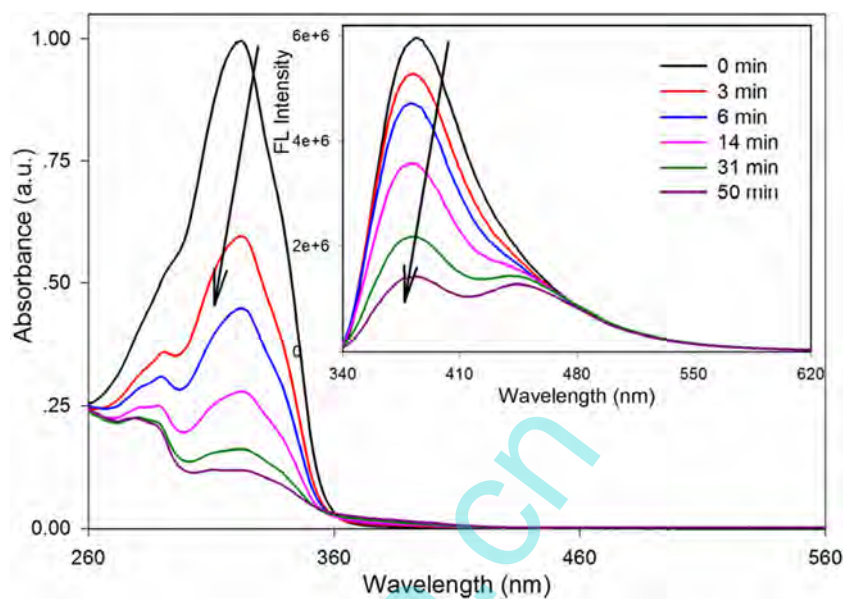


Fig. 3 Absorption and emission ($\lambda_{\text{ex}}=320$ nm) spectra of polymer aqueous solution (0.25 mg/mL \times 1 mL) upon 320 nm irradiation (0.86 mW/cm²)



micellar stability and the demands of the real-time UV–vis spectroscopy into consideration, the polymer aqueous solution used in the reversible photo-dimerization experiment was kept at 0.25 mg/mL.

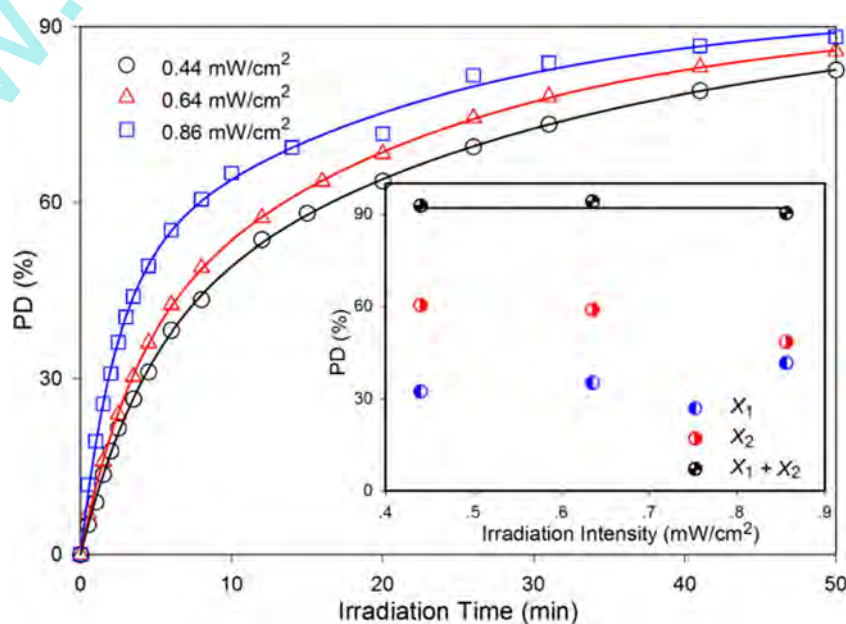
The photo-dimerization procedure upon 320 nm irradiation

Coumarin can be photo-dimerized upon irradiation at $\lambda > 300$ nm. As shown in Fig. 3, irradiation of polymer micelles with 320 nm light (0.86 mW/cm²) induced the photo-dimerization of coumarins and thus resulted in a gradual decrease in the absorption band at 320 nm. It is simple to understand that the photo-dimerization of coumarin pendants within polymer micelles may compact the loose micelles, thus

resulting in the mutual closeness of the remaining coumarin. Evidently, as shown in the inset of Fig. 3, the disappearance of emission band at 385 nm (I_1) was accompanied with the emergence of a relatively weak, but significant, emission band at 445 nm (I_2) along with the irradiation time, indicating the ongoing closeness of the remaining coumarins within photo-crosslinked polymer micelles.

Figure 4 showed the estimated PD values based on the absorbance changes of polymer micelles upon different intensity irradiations of 320 nm light. The time-dependant PD values for coumarins showed saturating behavior and synchronously decreased with the lowering of irradiation intensities. These observed PD changes were fit well with a biexponential equation:

Fig. 4 The time-dependent PD values of polymer aqueous solution (0.25 mg/mL \times 1 mL) upon 320 nm irradiations; the solid curves were four parameter biexponential fits to Eq. 2, and the inset showed the zero-order intensity dependence of $X_1 + X_2$ as a function of irradiation intensities



$$PD(t) = X_1(1 - e^{-k_1 t}) + X_2(1 - e^{-k_2 t}) \quad (2)$$

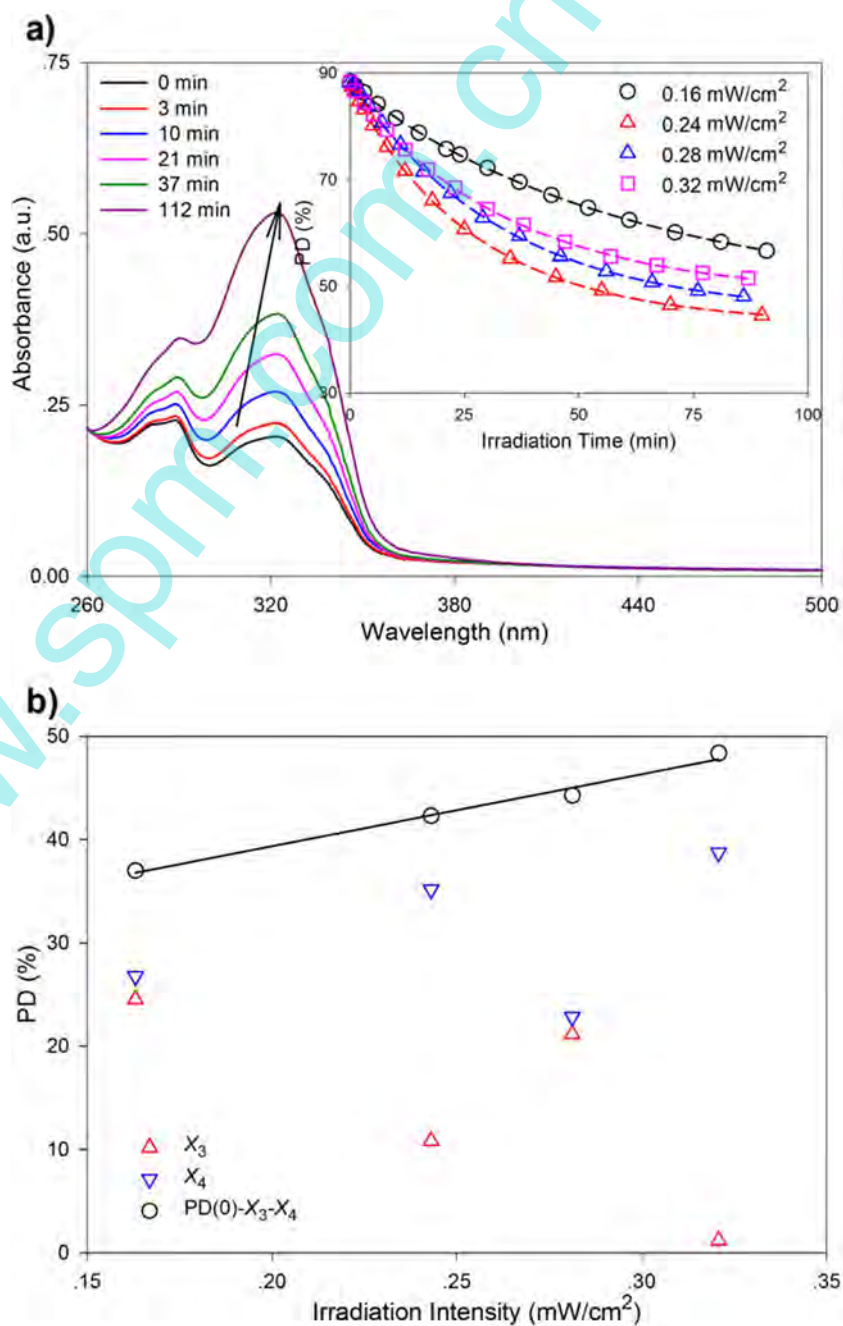
where $PD(t)$ corresponded to the time-dependent photo-dimerization degree, k_1 and k_2 were rate constants, and X_1 and X_2 were the relative weight fractions [31, 32]. To be emphasized, the sum of X_1 and X_2 determined the maximum photo-dimerization extent (PD_{\max}) that the coumarin pendants could reach after the long enough irradiation time [33]. As shown in the inset of Fig. 4, the obtained values of $X_1 + X_2$ at different irradiation intensities fluctuated weakly around 92 % and

afforded a good zero-order linear fit, indicating that PD_{\max} of coumarin pendants within polymer micelles upon 320 nm light irradiations was always intensity-independent at the used conditions.

The photo-reaction procedure upon 254 nm irradiation

The coumarin photo-dimers can also revert to the starting compound upon irradiation with shorter wavelength ($\lambda < 300$ nm) [31]. As designed, the polymer micelles were first irradiated by 320 nm light (0.86 mW/cm^2) to a given photo-

Fig. 5 **a** Absorbance spectra of photo-crosslinked polymer micelles ($0.25 \text{ mg/mL} \times 1 \text{ mL}$, $PD(0)=88.31 \%$) upon 254 nm light (0.24 mW/cm^2); the *inset* showed the time-dependent PD values of polymer micelles upon 254 nm irradiations, and the *solid curves* were four parameter biexponential fits to Eq. 3. **b** The intensity dependence of X_3 , X_4 and $PD(0)-X_3-X_4$ as a function of irradiation intensities



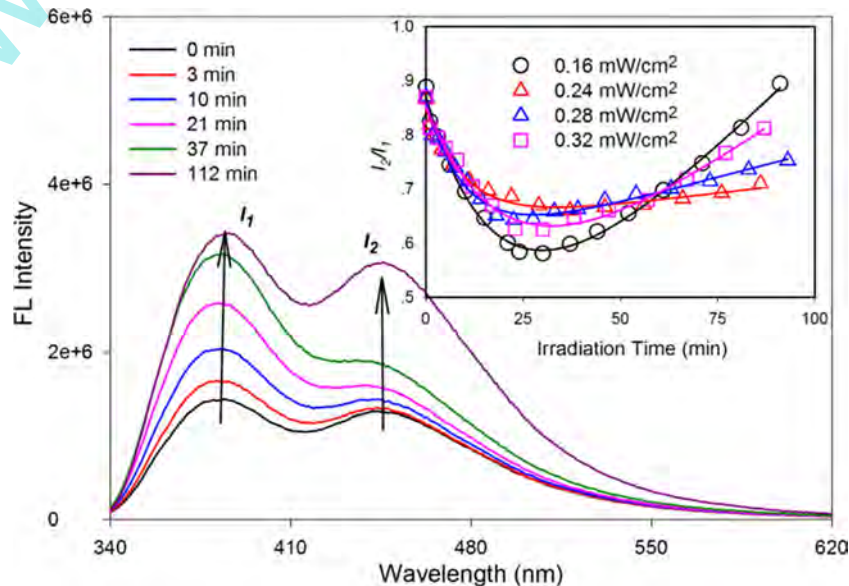
dimerization degree (88.31 %), then irradiated by 254 nm light. As shown in Fig. 5a, the absorbance at 320 nm recovered along with 254 nm irradiations (0.24 mW/cm^2), indicating the ongoing scission of the coumarin photo-dimers and resulting in the decline of PD values along with the irradiation time. The time dependences of these observed PD changes upon various intensity irradiations of 254 nm light were fit reasonably with a biexponential equation:

$$\text{PD}(t) = \text{PD}(0) - X_3(1 - e^{-k_3 t}) - X_4(1 - e^{-k_4 t}) \quad (3)$$

where $\text{PD}(t)$ corresponded to the PD value after t time of photo-cleavage, $\text{PD}(0)$ was the given PD value (88.31 %) of the photo-dimerized coumarin solution, k_3 and k_4 were rate constants, and X_3 and X_4 were the relative weight fractions. It is understandable that Eqs. 2 and 3 were opposite to each other since these two fitting equations were derived from the reversible photo-dimerization process of coumarin pendants within polymer micelles. Furthermore, $\text{PD}(0) - X_3 - X_4$ determined the maximum photo-cleavage (PC_{max}) that the system could reach after the long enough photo-dissociation time; the smaller the $\text{PD}(0) - X_3 - X_4$, the higher the PC_{max} . Figure 5b showed the linear fit of the obtained values of $\text{PD}(0) - X_3 - X_4$ at different irradiation intensities, indicating that the maximum photo-dissociation extent of coumarin photo-dimers declined linearly with the increasing intensity of 254 nm irradiations at the used conditions.

Figure 6 showed the emission spectra of the photo-crosslinked polymer micelles upon 254 nm irradiations; the first band at 385 nm (I_1) recovered quickly in the initial 40 min, then began to flatten, and conversely, the second band at 445 nm (I_2) increased slowly in the initial stage, then ascended rapidly in the remaining of the photo-dissociation procedure.

Fig. 6 Emission spectra of photo-crosslinked polymer micelles ($0.25 \text{ mg/mL} \times 1 \text{ mL}$, $\lambda_{\text{ex}} = 320 \text{ nm}$, $\text{PD}(0) = 88.31 \%$) upon 254 nm light (0.24 mW/cm^2); the inset showed the dependence of I_2/I_1 as a function of irradiation time



As shown in the inset of Fig. 6, the general time-dependent values of I_2/I_1 of polymer micelles upon different intensity irradiations of 254 nm light went down at first with an exponential decay and then went up to near the original, indicating the ongoing mutual closeness of coumarin pendants. Combining the I_2/I_1 ratio changes during the photo-dimerization procedure, it was very interesting that both the photo-dimerization and photo-dissociation resulted in the closeness of coumarin pendants within polymer micelles.

The reversible photo-dimerization cycles upon alternative irradiations

To further elucidate the dynamic hydrophobic association of coumarin pendants during the photo-dimerization and photo-dissociation stages, polymer aqueous solution ($0.25 \text{ mg/mL} \times 1 \text{ mL}$) was irradiated alternatively with 320 and 254 nm light. As shown in Fig. 7, when polymer solution was exposed to alternative irradiations of 320 nm (0.86 mW/cm^2 , 50 min) and 254 nm (0.24 mW/cm^2 , 90 min) for four cycles, the time-dependent PD values in every photo-dimerization procedure showed similar saturating behaviors with the final PD values at 88.3, 84.3, 82.8, and 82.6 % respectively, and the PD values in photo-cleavage stages decayed progressively with the final at 44.0, 59.5, 68.3, and 73.0 % respectively, resulting in the more compact micellar morphologies. At the same time, the I_2/I_1 ratios in every photo-dimerization procedure increased almost linearly and ended at 0.89, 2.54, 3.60, and 4.39 respectively, and the I_2/I_1 ratios in every photo-cleavage stage decayed exponentially with the final at 0.90, 1.52, 2.11, and 2.76 respectively. Those up-down changes of I_2/I_1 ratios announced that the coumarins were wavily speeding toward each other along with the irradiation cycles.

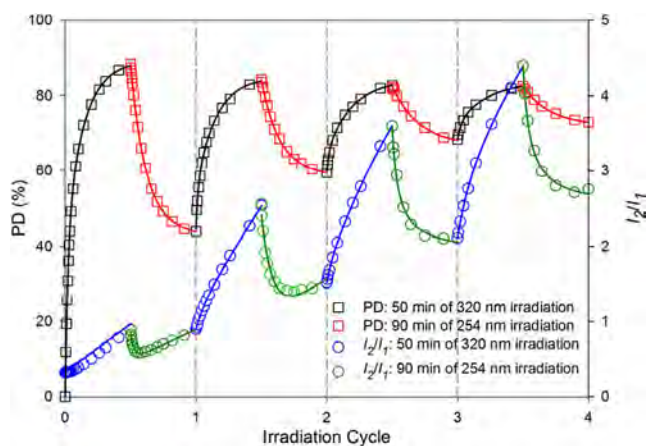


Fig. 7 PD and I_2/I_1 ratio changes of polymer aqueous solution ($0.25 \text{ mg/mL} \times 1 \text{ mL}$) upon alternative irradiations of 320 nm (0.86 mW/cm^2) and 254 nm (0.24 mW/cm^2)

It is known that the photo-dimerization of coumarin within polymer micelles would result in the cross-linking of polymer chains and, thus, the more compact micellar morphologies, which would predictably change the physicochemical parameters of polymer micelles, such as the micellar size and solution transmittance. However, when the above polymer aqueous solution upon alternative irradiation cycles was taken by the transmittance and micellar size analysis, there came no significant or efficient changes because of the too low polymer concentration at 0.25 mg/mL . Thus, a thicker polymer aqueous solution ($5.0 \text{ mg/mL} \times 1.5 \text{ mL}$) was alternatively irradiated by 320 nm (0.86 mW/cm^2 , 200 min) and 254 nm (0.24 mW/cm^2 , 150 min) for four cycles and simultaneously monitored by transmittance analysis and DLS instrument. As shown in Fig. 8a, when upon alternative irradiations, the micellar transmittance first dropped quickly from 87.9 to 82.6 %, then recovered gradually to 87.9 % in the remaining of the first photo-dimerization cycle; subsequently, it afforded a slow and progressive ascending from 87.9 to 90.2 % in the successive three photo-reaction stages and began to flatten in the remaining four stages of irradiation cycles. At the same time, as shown in Fig. 8b, the zeta average size of polymer micelles correspondingly decreased from 90.4 to 77.4 nm, then recovered to 84.4 nm in the first photo-dimerization stage, and then it afforded an alternative and slight increment and decrement in the subsequent photo-cleavage and photo-dimerization stages of irradiation cycles. The AFM pictures in the inset of Fig. 8b for polymer micelles in the first irradiation cycle showed uniformly spherical micelles (the details can be seen from S9, S10 and S11 in the Supporting Information). It seemed that the average diameter measured by AFM of polymer micelles before photo-dimerization (A, 60 nm) was slightly smaller than those after photo-dimerization (B, 90 nm) and after photo-dissociation (C, 80 nm) respectively. This is because the AFM samples were prepared with much more diluted polymer aqueous solutions ($2.50 \times 10^{-2} \text{ mg/mL}$), and

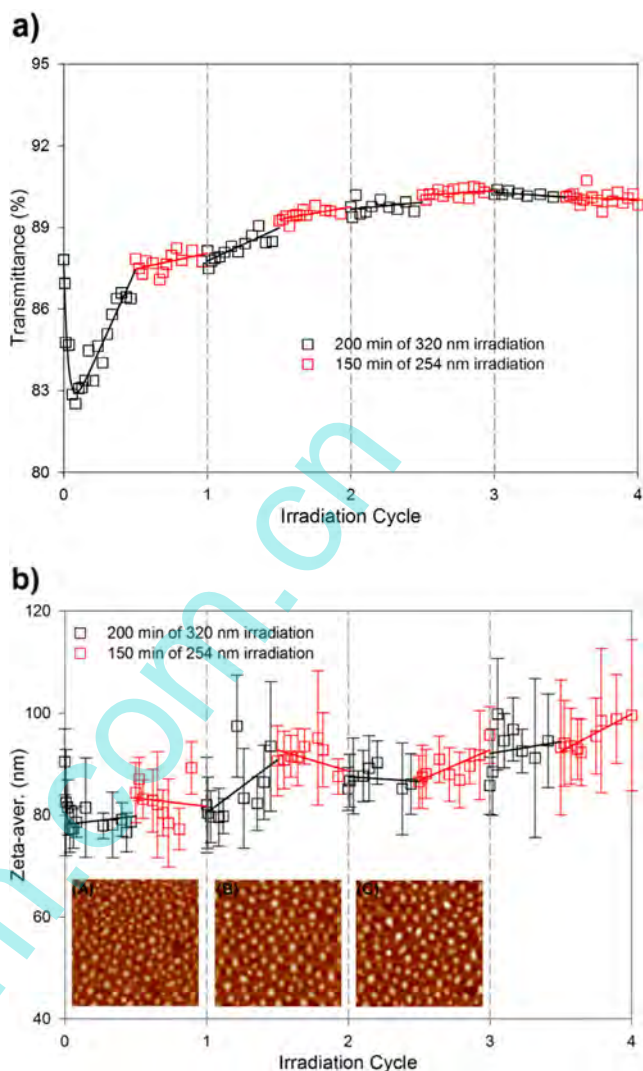


Fig. 8 Transmittance (a) and zeta average size (b) changes of polymer aqueous solution ($5.0 \text{ mg/mL} \times 1.5 \text{ mL}$) upon irradiation cycles of 320 nm (0.86 mW/cm^2) and 254 nm (0.24 mW/cm^2); AFM images ($2 \times 2 \mu\text{m}^2$) of polymer micelles before (A) and after (B) photo-dimerization and after photo-dissociation (C) in the first irradiation cycle

polymer micelles before photo-dimerization may reassemble into smaller nano-particles during the dilution, while the partially reversible photo-dimerization stabilizes the polymer micellar structure.

Conclusions

To summarize, we have synthesized a water-soluble amphiphilic random copolymer of P(DMA-*co*-VBC) with coumarin pendants, which could instantly form micelles in aqueous solution with hydrophobic coumarin pendants gradually associating from the outside to the inside. The alternative irradiation experiment at 320 and 254 nm showed that coumarin

pendants within polymer micelles can be reversibly photo-dimerized. Furthermore, the derived I_2/I_1 ratio changes based on emission bands at 445 nm (I_2) and 385 nm (I_1) during the reversible photo-dimerization cycles showed a wave-like increase as a function of irradiation cycles, indicating the dynamic closeness of coumarin pendants within polymer micelles.

Acknowledgments This work is supported by the Nature Science Foundation of China (NSFC 21374056), the Natural Science Basic Research Plan in Shaanxi Province of China (NSBRP-SPC 2014JM2051), the Fundamental Research Funds for the Central Universities (GK201302045), Shaanxi Innovative Research Team for Key Science and Technology (2012KCT-21, 2013KCT-17), and the One Hundred Plan of Shaanxi Province.

References

- Kotz J, Kosmella S, Beitz T (2001) Self-assembled polyelectrolyte systems. *Prog Polym Sci* 26:1199–1232
- Kim BS, Mather PT (2002) Amphiphilic telechelics incorporating polyhedral oligosilsesquioxane: 1. synthesis and characterization. *Macromolecules* 35:8378–8384
- Liu RCW, Pallier A, Brestaz M, Pantoustier N, Tribet C (2007) Impact of polymer microstructure on the self-assembly of amphiphilic polymers in aqueous solutions. *Macromolecules* 40:4276–4286
- Shi DJ, Matsusaki M, Akashi M (2009) Photo-crosslinking induces size change and stealth properties of water-dispersible cinnamic acid derivative nanoparticles. *Bioconjug Chem* 20:1917–1923
- Forder C, Patrickios CS, Armes SP, Billingham NC (1996) Synthesis and aqueous solution characterization of dihydrophilic block copolymers of methyl vinyl ether and methyl triethylene glycol vinyl ether. *Macromolecules* 29:8160–8169
- Peetla C, Graf K, Kressler J (2006) Langmuir monolayer and langmuir-blodgett films of amphiphilic triblock copolymers with water-soluble middle block. *Colloid Polym Sci* 285:27–37
- Coppola L, Oliviero C, Pogliani L, Ranieri GA, Terenzi M (2000) A self-diffusion study in aqueous solution and lyotropic mesophases of amphiphilic block copolymers. *Colloid Polym Sci* 278:434–442
- Kim KM, Choi S, Jeon HJ, Lee JY, Choo DJ, Kim J (2008) Synthesis of new pH-sensitive amphiphilic block copolymers and study for the micellization using a fluorescence probe. *Macromol Res* 16:169–177
- Garofalo C, Capuano G, Sottile R, Tallerico R, Adami R, Reverchon E, Carbone E, Izzo L, Pappalardo D (2014) Different insight into amphiphilic PEG-PLA copolymers: influence of macromolecular architecture on the micelle formation and cellular uptake. *Biomacromolecules* 15:403–415
- Hafezi MJ, Sharif F (2012) Brownian dynamics simulation of micellization of amphiphilic block copolymers with different tail lengths. *Langmuir* 28:16243–16253
- Zhunuspayev DE, Mun GA, Khutoryanskiy VV (2010) Temperature-responsive properties and drug solubilization capacity of amphiphilic copolymers based on N-vinylpyrrolidone and vinyl propyl ether. *Langmuir* 26:7590–7597
- Sutton D, Nasongkla N, Blanco E, Gao JM (2007) Functionalized micellar systems for cancer targeted drug delivery. *Pharm Res* 24:1029–1046
- Nowakowska M, Karewicz A, Klos M, Zapotoczny S (2003) Synthesis and properties of water-soluble poly(sodiumstyrenesulfonate-block-5-(4-acryloyloxyphenyl)-10, 15, 20-tritoyl porphyrin) by nitroxide-mediated free radical polymerization. *Macromolecules* 36:4134–4139
- Jiang JQ, Shu QZ, Chen X, Yang YQ, Yi CL, Song XQ, Liu XY, Chen MQ (2010) Photoinduced morphology switching of polymer nanoaggregates in aqueous solution. *Langmuir* 26:14247–14254
- Trenor SR, Shultz AR, Love BJ, Long TE (2004) Coumarins in polymers: from light harvesting to photo-cross-linkable tissue scaffolds. *Chem Rev* 104:3059–3078
- Alvarez TMG, Devi LS, Russell MM, Schwartz BJ, Zink JI (2013) Activation of snap-top capped mesoporous silica nanocontainers using two near-infrared photons. *J Am Chem Soc* 135:14000–14003
- Rabnawaz M, Liu GJ (2014) Triblock copolymers bearing a redox-cleavable junction and a photo-cross-linkable block. *Macromolecules* 47:5115–5123
- Jin Q, Mitschang F, Agarwal S (2011) Biocompatible drug delivery system for photo-triggered controlled release of 5-fluorouracil. *Biomacromolecules* 12:3684–3691
- Ciamician G, Silber P, Ber D (1902) Giacomo ciamician und P. silber: chemische lichtwirkungen. *Chem Ges* 35:4128–4131
- Mal NK, Fujiwara M, Tanaka Y (2003) Photocontrolled reversible release of guest molecules from coumarin-modified mesoporous silica. *Nature* 421:350–353
- Jiang JQ, Qi B, Lepage M, Zhao Y (2007) Polymer micelles stabilization on demand through reversible photo-cross-linking. *Macromolecules* 40:790–792
- He J, Yan B, Tremblay L, Zhao Y (2011) Both core- and shell-cross-linked nanogels: photo-induced size change, intraparticle LCST, and interparticle UCST thermal behaviors. *Langmuir* 27:436–444
- Guo ZX, Jiao TF, Liu MH (2007) Effect of substituent position in coumarin derivatives on the interfacial assembly: reversible photodimerization and supramolecular chirality. *Langmuir* 23:1824–1829
- Schadt M, Seiberle H, Schuster A (1996) Optical patterning of multidomain liquid-crystal displays with wide viewing angles. *Nature* 381:212–215
- Schrauba M, Soll S, Hampp N (2013) High refractive index coumarin-based photorefractive polysiloxanes. *Eur Polym J* 49:1714–1721
- Jiang JQ, Feng Y, Wang HM, Liu XY, Zhang SW, Chen MQ (2008) Synthesis and micellization of photosensitive amphiphilic comblike SMA polymer. *Acta Phys -Chim Sin* 24:2089–2095
- Fu Q, Cheng LL, Zhang Y, Shi WF (2008) Preparation and reversible photo-crosslinking/photo-cleavage behavior of 4-methylcoumarin functionalized hyperbranched polyester. *Polymer* 49:4981–4988
- Ananthapadmanabhan KP, Goddard ED, Goddard D, Turro NJ, Kuo PL (1985) Fluorescence probes for critical micelle concentration determination. *Langmuir* 1:352–355
- Lin Y, Alexandridis P (2002) Cosolvent effects on the micellization of an amphiphilic siloxane graft copolymer in aqueous solutions. *Langmuir* 18:4220–4231
- Nivaggioli T, Alexandridis P, Hatton TA, Yekta A, Winnik MA (1995) Fluorescence probe studies of pluronic copolymer solutions as a function of temperature. *Langmuir* 11:730–737
- Liu Y, Chang H, Jiang JQ, Yan XY, Liu ZT, Liu ZW (2014) The photodimerization characteristics of anthracene pendants within amphiphilic polymer micelles in aqueous solution. *RSC Adv* 4:25912–25915
- Jezowski SR, Zhu LY, Wang YB, Rice AP, Scott GW, Bardeen CJ, Chronister EL, Chronister EL (2012) Pressure catalyzed bond dissociation in an anthracene cyclophane photodimer. *J Am Chem Soc* 134:7459–7466
- Daniel K, Peter BR, Cheol KH, Norbert H (2011) Photochemistry of coumarin-functionalized SiO₂ nanoparticles. *Langmuir* 27:4149–4155